Sensitivity analysis of residuals for soft fault monitoring in Y-shaped networks

Abdelkarim Abdelkarim, Virginie Degardin, Vincent Cocquempot

Sensitivity analysis of residuals for soft fault monitoring in Y-shaped networks

Abdel Karim Abdel Karim
UMR 9189 - CRIStAL, UMR 8520 - IEMN
University of Lille
F-59000 Lille, France
abdel-karim.abdel-karim@univ-lille.fr

Degardin Virginie
UMR 8520 - IEMN
University of Lille
F-59000 Lille, France
virginie.degardin@univ-lille.fr

Cocquempot Vincent
UMR 9189 - CRIStAL
University of Lille
F-59000 Lille, France
vincent.cocquempot@univ-lille.fr

***Abstract*—Networks, mainly composed of cables, are prone to failures. Faults in cables are initially benign (so-called soft faults) and then evolve over time to a much more severe form of faults as short or open circuits (so-called hard faults). It is thus of prime importance to detect and localize efficiently the soft faults. Residuals may be calculated by comparing online computed transmission coefficients with reference transmission coefficients. In this paper, the sensitivity of the residuals with respect to the fault is studied for a simulated but realistic Y-shaped network. The residuals are represented in the residuals space. Using intensive simulations, the residuals are analyzed with respect to the position of the fault in a branch, the severity of the fault and the signal-to-noise ratio.**

***Index Terms*—Soft fault, Sensitivity analysis, Fault monitoring, Electrical cables, Power Line Communication.**

I. Introduction

Electrical cables are omnipresent to transfer data or energy in technological systems. These cables are subject to degradation or faults e.g. humidity in a submarine can cause water-treeing [5], mechanical stress can cause insulation cuts [17] etc .... These degradation or faults are considered as *soft faults* if the cables are still able to provide power or data, and once that transmission is interrupted, they are considered as *hard fault*s. Hard faults (short-circuit, open circuit) are the faults that led to the TWA 800 (in 1996) and Swissair 111 (in 1998) tragedies [11]. Hence, a monitoring system that is capable of detecting soft faults in networks before they turn into hard faults, is needed. The most used fault detection and localization methods in the literature are based on time domain reflectometry or frequency domain reflectometry [12]. A review of existing reflectometry-based methods is conducted in [13]. Almost all reflectometry-based methods can detect and locate hard faults without problems. However, they are limited when it comes to detecting soft faults especially online [16], [22]. These methods are based on the analysis of the waves reflected back to the injection port (the source side). Alternative methods propose the analysis of the waves received by the receiver side as in [14] and [15]. These alternative methods are based on the comparison between the reference transmission coefficients of the network estimated when the network is considered in the no-fault situation and those estimated online. The estimation of the transmission coefficients can be done online by the installed Electronic Control Unit (ECU) through Orthogonal Frequency Division Multiplexing (OFDM) using the Power Line Communication (PLC) technique [6], without using additional instruments or sensors.

In [3], [4], residuals based on the transmission coefficients were proposed. It was theoretically shown that these residuals equal zero in no-fault situation and are different from zero in presence of soft faults. They can thus be used to detect the faults. Residuals may be computed for different couples of receivers and sources leading to a set of structured residuals. The obtained residual signature allows not only the detection of the fault but also the localization of the faulty branch in a network. The method was tested on a real test bench and the results were reported in [2].

Since it is physically impossible to test a physical network in many different faulty situations, simulation-based data are needed to study the sensitivity of the residuals. The transmission chain model [10], [18] is a well-known model that can be used to simulate the signal transmission in a network with great accuracy, if the targeted network characteristics (topology, load impedance, physical characteristics of the cable) are perfectly known. It is reported in the literature that the simulated data and the test bench data match each other not only when the network is non-faulty [19] but also in different fault situations where the faults are simulated as additive impedance [20].

The main contribution of this paper is the study of the sensitivity of the residuals with respect to :

- The position of the fault on a branch.
- The fault amplitude for a given position.
- The level of the noise on the transmission coefficients.

Intensive simulations of the transmission chain model are performed to analyse the impact of the characteristics of the soft faults (position and amplitude) on the residuals. Due to the presence of noise, for a given fault characteristic, the residuals form a distribution represented by a cluster in the residuals space. The Mahalanobis distance between each sample and a reference cluster is used to study the influence of the faults and of the environment noise on the residuals.

This research work is done in the framework of the ELSAT2020 project which is co-financed by the European Union with the European Regional Development Fund, the French state and the Hauts-de-France Region Council.

This paper is organized as follows. In section II, the fault detection method based on the transmission coefficients is briefly described, along with the studied Y-shaped transmission network. In section III, the data generation procedure and the analysis of the obtained clusters are detailed. Then, in section IV, the sensitivity of the residuals is analysed with respect to the position of the fault, its severity and the level of the additive noise. Conclusions and future work close this paper.

II. Background

A. Network and residuals

The studied network is a Y-shaped network as shown in Fig. 1. It is composed of one node, three branches B_i and three electronic control units ECU_i (with $i \in \{0;1;2\}$). Each ECU acts either as a source S_i or as a receiver R_i. This network is shown in its no-fault situation (all branches are fault free), and its three possible faulty situations (A fault is on one of the three branches). Note that the multiple faults case is outside the scope of this paper.

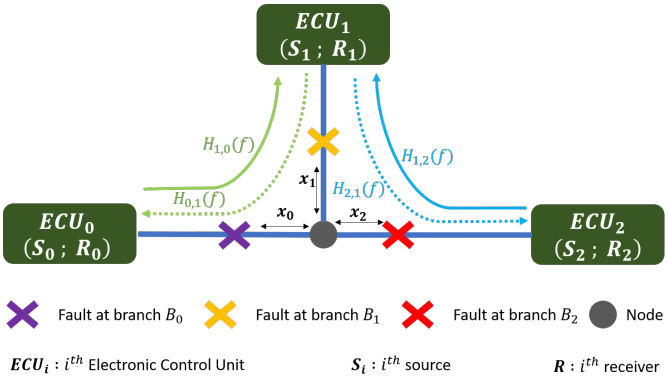

Fig. 1: Y-shaped network.

Remark 1. *A Y-shaped network is considered here, but the monitoring method is easily usable for other networks topologies, as a complex network can always be decomposed into several Y-shaped subnetworks.*

In real life application, thanks to the power line communication (PLC) technology, the transmission coefficient, denoted $H_{j,i}(f)$, between a source S_i and a receiver R_j can be estimated through orthogonal frequency division multiplexing (OFDM) process by each receiver (f denotes the frequency). In [2], it was shown that $H_{j,i}(f)$ is theoretically sensitive to the fault. In a Y-shaped network, two transmission coefficients per receiver can be estimated resulting in six transmission coefficients. Health indicators based on those transmission coefficients are proposed to detect a fault.

Definition 1. *Health indicators, denoted $I_{j,i}(f)$, are defined by the following expression*

$$I_{j,i}(f) = \left| \frac{H_{j,i}^{Reference}(f)}{H_{j,i}(f)} \right| - 1 \tag{1}$$

where $H_{j,i}^{Reference}(f)$ is the transmission coefficient between the source S_i and the receiver R_j estimated when the network is considered in the no-fault situation and $H_{j,i}(f)$ is the transmission coefficient that is estimated online.

Remark 2. *In total, six health indicators can be computed for a Y-shaped network. However, it will be shown in the following that only four indicators are needed to detect and locate the faulty branch. To reduce the computation and communication costs only four among the six health indicators are thus computed.*

Residuals, denoted r_i, based on these health indicators are proposed to distinguish between the no-fault and faulty situation of the network.

Definition 2. *A residual, r_i, is defined by the following expression*

$$r_i = \frac{1}{N} \sum_{f=f_1}^{f=f_N} |I_{j,i}(f) - I_{l,i}(f)| \tag{2}$$

with $f \in BW = [f_1 : f_N]$. BW is the bandwidth of interest that starts from the frequency f_1 and ends at the frequency f_N, N is the number of frequency components. i is the index of the ECU acting as the source, j and l are the indices of the ECU acting as the receivers with $i \neq j \neq l$.

A residual per ECU acting as a source is computed resulting in three residuals. However, only two residuals are needed to get different residual fault signatures, the third residual is a redundant residual. The expressions of r_0 and r_1 are

$$r_0 = \frac{1}{N} \sum_{f=f_1}^{f=f_N} |I_{1,0}(f) - I_{2,0}(f)| \tag{3}$$

$$r_1 = \frac{1}{N} \sum_{f=f_1}^{f=f_N} |I_{0,1}(f) - I_{2,1}(f)| \tag{4}$$

It has been shown in [1]–[4] that the residuals are theoretically sensitive to faults and they can be used to detect faults and to locate the faulty branch using the signature matrix shown in Table I. The columns of this signature matrix represent the four situations of the network namely, no-fault situation, faulty B_0, faulty B_1 and faulty B_2. The rows represent the residuals r_0 and r_1 respectively computed at the sources S_0 and S_1. All residuals fault signatures are different which shows that it is possible to identify the faulty situation with only two residuals.

TABLE I: Signature matrix of the residuals.

r_i	No-fault	Faulty B_0	Faulty B_1	Faulty B_2
r_0	0	0	1	1
r_1	0	1	0	1

0 indicates that r_i is equal to zero.
1 indicates that r_i is different from zero.

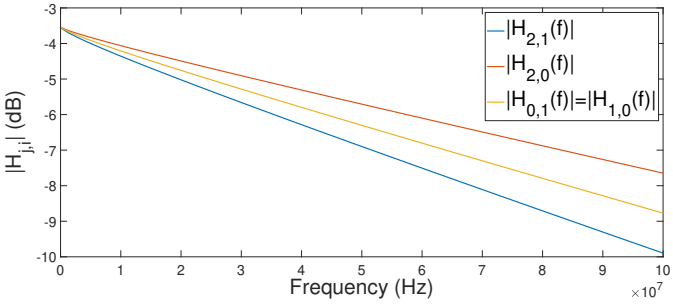

Fig. 2: Module of the transmission coefficients.

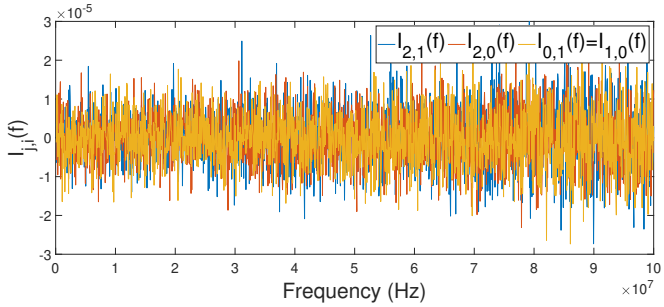

Fig. 3: Health indicators.

B. Residual computation method

The residual computation method consists of three steps :

1) Step 1 : In a physical network, the transmission coefficients $H_{j,i}(f)$ are estimated online at the j^{th} receiver through OFDM process sent by the i^{th} source in the bandwidth of interest BW [7]. As previously mentioned, in this paper, intensive simulations of the transmission chain model are performed, thus the $H_{j,i}(f)$ values are directly given (see Fig. 2).
2) Step 2 : The indicators $I_{j,i}(f)$ are computed at the receiver R_j then they are sent to the source S_i via PLC link (see Fig. 3).
3) Step 3 : The residuals r_i are computed at the source S_i and plotted in the residuals space.

A point (r_0, r_1) in the residuals space represents the state of the network. Depending on the position of the point, the fault is detected and the faulty branch is located. This computation method was applied, in [4] and in [2], using actual data extracted from a test bench and simulated data but without looking at the influence of noise, the position of the fault in a branch and the severity of the fault. Since it is not physically possible to repeatedly change the position, the severity of the fault and the noise level on a real test bench, intensive simulations are performed to generate data. The next section will be dedicated to data generation and the influence of changing the fault and noise characteristics on the residuals.

III. Data generation and cluster analysis

A. Data set generation

The network shown in Fig. 1 is simulated via MATLAB using the chain matrix model [18]. As argued in the introduction section, the simulation is preferred here to be able to generate data in many different faulty situations, with the objective to study the sensitivity/robustness of the residuals. Soft faults are represented in simulations by the insertion of an impedance in series. The relevance of this representation was confirmed in [20], where real data and simulated ones were found to be consistent.

The primary parameters of the network R, L, C and G, needed to simulate the network, are computed using the analytical equations found in [9], [21]. R, L, C and G denote respectively the resistance, inductance, capacitance and conductance per unit length of the network. The lengths of the branches B_0, B_1 and B_2 are respectively $l_0 = 4\ m$, $l_1 = 10\ m$ and $l_2 = 7\ m$. The characteristic impedance, Z_c, of each branch is equal to 120Ω. A soft fault is defined as a small change in the local impedance of the cable, it is represented in simulations by the insertion of an impedance Z_f in series [20].

B. Data set representation in the residuals space

As an illustration, the following example with fixed fault and noise characteristics is considered. The four situations of the network are considered by fixing the signal-to-noise ratio (SNR) to 100 dB in both no-fault and faulty situations. In the faulty situations, the fault severity Z_f is fixed to 5 Ω and the distance between the fault and the node is fixed to $x_i = 1\ m$. The generated data are :

- The transmission coefficients, $H_{1,0}(f)$ and $H_{2,0}(f)$, between the source S_0 and the receivers R_1 and R_2.
- The transmission coefficients, $H_{0,1}(f)$ and $H_{2,1}(f)$, between the source S_1 and the receivers R_0 and R_2.

Using those two couples of transmission coefficients, the two residuals r_0 and r_1 are computed. These residuals are represented in the residuals space. The three steps presented in the sub-section II-B are repeated 100 times in the no-fault situation of the network resulting in 100 points in the residuals space. Due to the noise, the 100 points form a cluster.

Remark 3. *In a no-fault situation, the points representing the residuals should vary around zero. Due to the non-linear character of the residual, the residuals are not around zero. To simplify the fault monitoring procedure, the mean values of the residuals in the no-fault situation* (ν_0, ν_1) *are subtracted from the computed residuals. As a consequence, the new set of points becomes centered around zero in the no-fault situation (green points in Fig.4).* ν_0 *and* ν_1 *are subtracted to each couple of computed residuals in the following.*

To illustrate the construction of clusters according to the situation of the network, the same steps are repeated also for each faulty situation. The resulting clusters are presented in Fig. 5 and they are consistent with Table I.

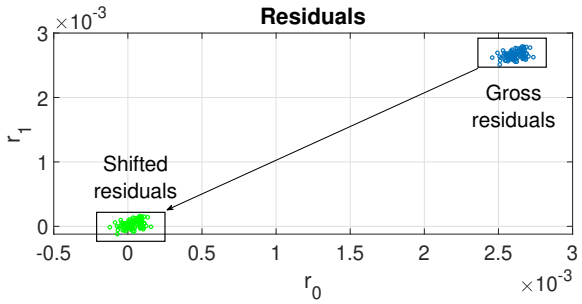

Fig. 4: Residuals in no-fault situation.

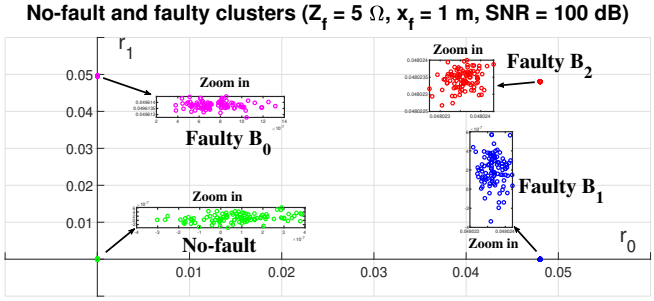

Fig. 5: No-fault and faulty clusters.

1) The no-fault situation represented by a green cluster centered at (0,0) ($r_0 = 0; r_1 = 0$).
2) Faulty B_0 represented by a magenta cluster located at the r_1-axis ($r_0 = 0$; $r_1 \neq 0$).
3) Faulty B_1 represented by a blue cluster located at the r_0-axis ($r_0 \neq 0$; $r_1 = 0$).
4) Faulty B_2 represented by a red cluster located in the plan formed by r_0 and r_1 ($r_0 \neq 0$; $r_1 \neq 0$).

To study the influence of the fault and noise characteristics on the residuals, the distance between the reference cluster in green and each new sample is computed. The distance between a sample and a Gaussian distribution may be evaluated using the Mahalanobis distance [8]. Henceforth, half of the green cluster (50 points) is considered as the reference cluster, Z_{ref}, and the distance between each new sample, z_k, and this cluster will be computed using the Mahalanobis distance, MD. Instead of monitoring r_0 and r_1, MD will be monitored.

$$MD(k) = \sqrt{(z_k - \overline{Z_{ref}})^T \cdot C_{Z_{ref}}^{-1} \cdot (z_k - \overline{Z_{ref}})} \quad (5)$$

where Z_{ref} is the data matrix containing 50 reference samples in the rows computed for the two residuals r_0 and r_1 in the columns. $\overline{Z_{ref}}$ and $C_{Z_{ref}}^{-1}$ denote respectively the mean value and the variance–covariance matrix of Z_{ref}. z_k is the k^{th} sample whose distance from the reference cluster is calculated ($z_k = [r_0, r_1]_k$). The transposed matrix is indicated by ^{T}.

Remark 4. *In a Y-shaped network, two residuals are monitored. In more complex networks, a larger number of residuals is required, making it challenging to track the variation of all residuals. Monitoring the MD reduces the dimension of the problem and thus simplifies the decision making.*

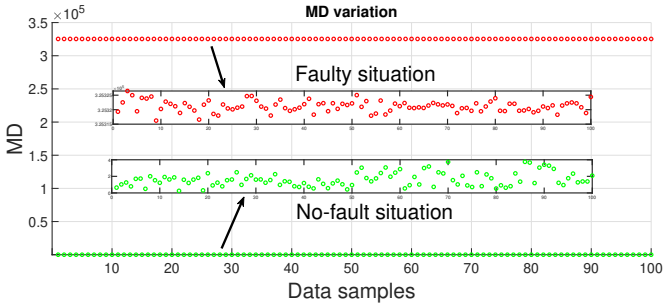

Fig. 6: Mahalanobis distance for faulty $B0$ state and no-fault situation.

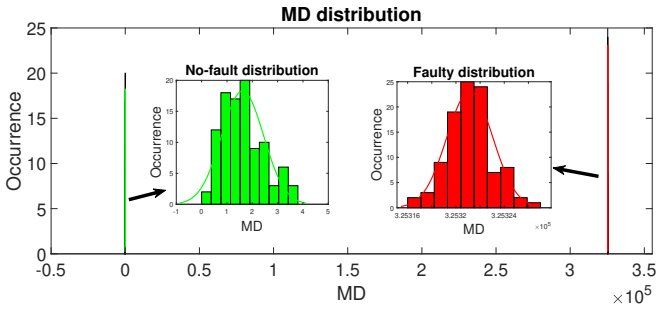

Fig. 7: Mahalanobis distribution for faulty $B0$ and no-fault situation.

The MD between the reference cluster, Z_{ref}, and each sample, z_i, in no-fault situation and in faulty B_0 situation are computed and shown in Fig.6. The distributions of the distances between the reference cluster and the samples in the no-fault and in the faulty B_0 situations are shown in Fig. 7.

In the next section, the evolutions of the clusters and the MD are studied with respect to the fault severity Z_f, the distance between the fault position and the node x and the signal-to-noise ratio (SNR) when an additive white Gaussian (AWG) noise is added to the transmission coefficients.

IV. Cluster Distance Analysis

Three characteristics, namely x_i, Z_f and SNR, can change either the cluster size or its distance from the reference cluster. A separate analysis of the influence of each of them is made in the following subsections where intensive simulations are performed by changing :

- The severity of the fault Z_f from 0.1 Ω to 15 Ω with a step of 0.1 Ω.
- The distance between the position of the fault and the position of the node x_i from 0.1 m to l_i m with a step of 0.1 m.
- The level of the noise that is added to the simulated transmission coefficients where the SNR varies from 0 dB to 50 dB with a step of 10 dB.

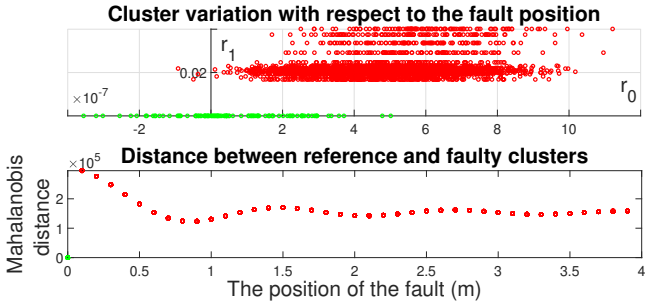

Fig. 8: Effect of the position of the fault (Faulty B_0).

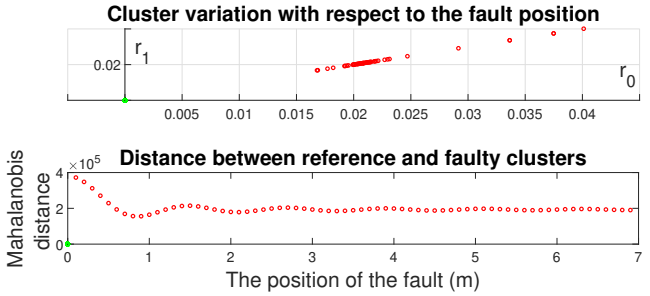

Fig. 9: Effect of the position of the fault (Faulty B_2).

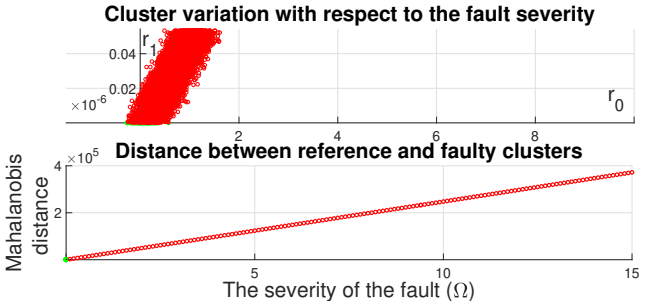

Fig. 10: Effect of the severity of the fault (Faulty B_0).

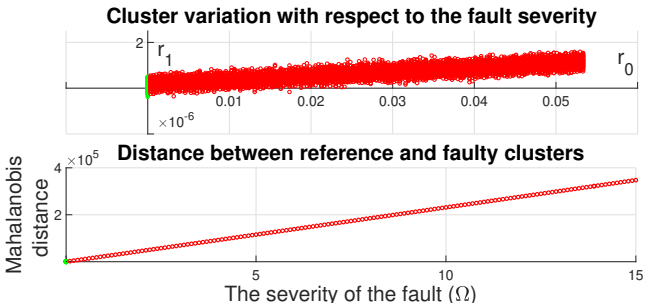

Fig. 11: Effect of the severity of the fault (Faulty B_1).

A. *Influence of the position of the fault*

Intensive simulation are performed while changing the distance, x_i, between the position of the fault and that of the node in each branch B_i.

The severity of the fault and the SNR are fixed respectively to $Z_f = 5\ \Omega$ and $SNR = 100\ dB$. Two faulty situations, B_0 and B_2, of the network are explored separately.

1) Faulty B_0: The distance, x_0, between the fault position and that of the node varies between $0.1\ m$ and $3.9\ m$ with a step of $0.1\ m$ resulting in 400 clusters. Each cluster is composed of 100 points. Each point represents the values of the residuals r_0 and r_1. The results are reported in Fig.8 where a faulty cluster is represented in red, and the no-fault cluster is represented in green. As it can be seen, the distance is maximum when the fault is close to the node, the distance is quite constant for all $x_0 > 0.5m$.

2) Faulty B_2: The same procedure as before is repeated by inserting a fault in the branch B_2 and by changing the distance, x_2, from $0.1\ m$ to $7\ m$. The red faulty clusters and the no-fault green cluster are represented in Fig. 9. As in the previous faulty situation, the MD is maximum when the fault is close to the node, and it is quite constant for all $x_0 > 0.5m$.

Conclusion : When the position of the fault in a branch is greater than $0.5\ m$ from the node, this position has quite no influence on the residuals. The fault influence on the residual grows when the fault approaches the node.

B. *Influence of the severity of the fault*

In this subsection, the fault position is fixed at $1\ m$ from the node while the SNR equals $100\ dB$. Two faulty situations of the network, faulty B_0 and faulty B_1, are discussed in the following.

1) Faulty B_0: The severity of the fault is increased from $0.1\ \Omega$ to $15\ \Omega$ with a step of $0.1\ \Omega$, the other two variables (x_0 and SNR) are fixed. The results are reported in Fig 10. As it can be seen, the faulty clusters deviate from the no-fault green cluster as a function of the fault severity and the distance between the faulty cluster and the no-fault cluster also increases linearly with the fault severity.

2) Faulty B_1: The same procedure is repeated with a fault in the branch B_1. As in the previous case, the distance between a faulty cluster and the no-fault cluster depends on the fault severity and it increases linearly as shown in Fig. 11. The difference between the two situations is the direction of the evolution of the clusters, as expected by the signature matrix shown in Table I. In faulty B_0, the clusters evolve in a direction following the r_1 axis. If the fault is in B_1 the clusters evolve in a direction following the r_0 axis.

Conclusion : The severity of the fault has a linear influence on the residuals which can be used to estimate the severity of the fault. The direction of this evolution depends on the faulty branch, as it is expected by the structured fault signature matrix (Table I).

C. *Influence of the signal-to-noise ratio*

In this subsection, both the severity of the fault and its distance from the node are fixed respectively at $5\ \Omega$ and at $1\ m$. The SNR changes from $0\ dB$ to $50\ dB$ with a step of $10\ dB$. Two of the faulty situations of the network, faulty B_0 and faulty B_1, are considered in what follows.

The results are reported in Fig.12 and Fig.13. As it can be

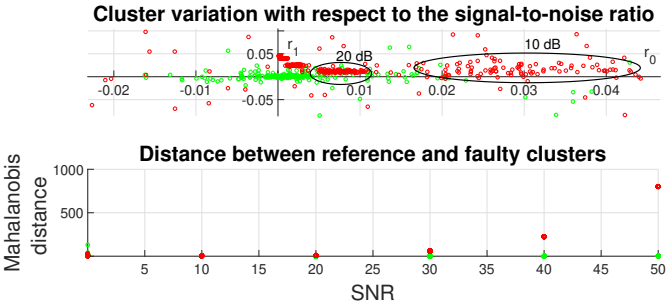

Fig. 12: Effect of the noise on the clusters (Faulty B_0).

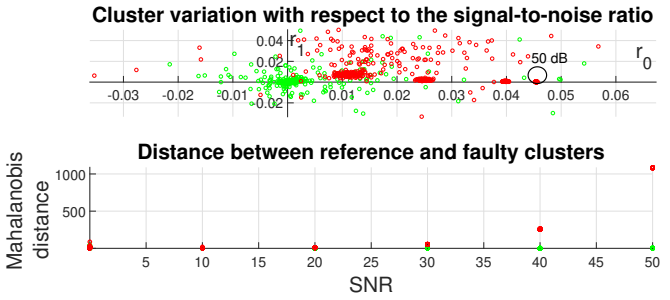

Fig. 13: Effect of the noise on the clusters (Faulty B_1).

seen, the cluster size increases with the level of noise. The distance between the no-fault cluster and the faulty cluster also decreases with the noise level (when increasing the SNR).
Conclusion : By decreasing the SNR value, the reference and the faulty clusters representing the residuals are increasing and may overlap, making it difficult to differentiate between them.

V. Conclusion and Future Work

In this paper, the sensitivity/robustness of the residuals for the detection of soft faults in Y-shaped networks is analyzed using intensive simulations. The influence of the fault position, the fault severity and the noise level on the residuals is studied. These residuals are represented as clusters in the residuals space. The Mahalanobis distance is used as a criterion to compare non-faulty and faulty data sets. It is concluded that the size of a cluster and its distance from the reference cluster depend on the severity of the fault and the noise level. The position of the fault has a limited influence on the clusters. These results may be used in future work to estimate the severity of the fault along the time. A minimum detectable fault for a given SNR can also be computed. In order to improve the localization decision, a residual per source can also be computed and represented in the residuals space.

References

[1] Abdel Karim, A.K., Atoui, A.M., Degardin, V., Cocquempot, V.: Fault detection and localization in vehicular embedded network using power line communication. In: 2021 9th International Conference on Systems and Control (ICSC). pp. 119–126. IEEE (2021)

[2] Abdel Karim, A.K., Atoui, A.M., Degardin, V., Cocquempot, V.: Fault detection and localization in y-shaped network through power line communication. In: 2021 5th International Conference on Control and Fault-Tolerant Systems (SysTol). pp. 103–108. IEEE (2021)

[3] Abdel Karim, A.K., Atoui, A.M., Degardin, V., Cocquempot, V.: Using power line communication for fault detection and localization in star-shaped network. In: 2022 11th IFAC Symposium on Fault Detection, Supervision and Safety for Technical Processes - SAFEPROCESS. IFAC (2022)

[4] Abdel Karim, A.K., Degardin, V., Cocquempot, V., Atoui, A.M.: Soft fault detection and localization in an unshielded twisted pair network using power line communication. In: 2021 7th International Conference on Vehicle Technology and Intelligent Transport Systems (VEHITS) (2021)

[5] Bulinski, A., Bamji, S., Densley, R.: The effects of frequency and temperature on water tree degradation of miniature xlpe cables. IEEE transactions on electrical insulation (4), 645–650 (1986)

[6] Cimini, L.: Analysis and simulation of a digital mobile channel using orthogonal frequency division multiplexing. IEEE transactions on communications **33**(7), 665–675 (1985)

[7] Coleri, S., Ergen, M., Puri, A., Bahai, A.: Channel estimation techniques based on pilot arrangement in ofdm systems. IEEE Transactions on broadcasting **48**(3), 223–229 (2002)

[8] De Maesschalck, R., Jouan-Rimbaud, D., Massart, D.L.: The mahalanobis distance. Chemometrics and intelligent laboratory systems **50**(1), 1–18 (2000)

[9] El Sahmarany, L.: Méthodes d'amélioration pour le diagnostic de câble par réflectométrie. Ph.D. thesis, Université Blaise Pascal-Clermont-Ferrand II (2013)

[10] Esmailian, T., Kschischang, F.R., Glenn Gulak, P.: In-building power lines as high-speed communication channels: channel characterization and a test channel ensemble. International Journal of Communication Systems **16**(5), 381–400 (2003)

[11] Furse, C., Haupt, R.: Down to the wire [aircraft wiring]. IEEE spectrum **38**(2), 34–39 (2001)

[12] Furse, C., Kamdar, N.: An inexpensive distance measuring system for navigation of robotic vehicles. Microwave and Optical Technology Letters **33**(2), 84–87 (2002)

[13] Furse, C.M., Kafal, M., Razzaghi, R., Shin, Y.J.: Fault diagnosis for electrical systems and power networks: A review. IEEE Sensors Journal **21**(2), 888–906 (2020)

[14] Huo, Y., Prasad, G., Atanackovic, L., Lampe, L., Leung, V.C.: Grid surveillance and diagnostics using power line communications. In: 2018 IEEE International Symposium on Power Line Communications and its Applications (ISPLC). pp. 1–6. IEEE (2018)

[15] Huo, Y., Prasad, G., Lampe, L., Leung, V.C., Vijay, R., Prabhakar, T.: Measurement aided training of machine learning techniques for fault detection using plc signals. In: 2021 IEEE International Symposium on Power Line Communications and its Applications (ISPLC). pp. 78–83. IEEE (2021)

[16] Lee, H.M., Lee, G.S., Kwon, G.Y., Bang, S.S., Shin, Y.J.: Industrial applications of cable diagnostics and monitoring cables via time–frequency domain reflectometry. IEEE Sensors Journal **21**(2), 1082–1091 (2020)

[17] Lundquist, E.J., Nagel, J.R., Wu, S., Jones, B., Furse, C.: Advanced forward methods for complex wire fault modeling. IEEE Sensors Journal **13**(4), 1172–1179 (2012)

[18] Meng, H., Chen, S., Guan, Y., Law, C., So, P., Gunawan, E., Lie, T.: Modeling of transfer characteristics for the broadband power line communication channel. IEEE Transactions on Power delivery **19**(3), 1057–1064 (2004)

[19] Nizigiyimana, R., Le Bunetel, J.C., Raingeaud, Y., Ravier, P., Lamarque, G., Achouri, A.: Analysis and comparison of deterministic power line channel modeling methods. International Journal on Communications Antenna and Propagation **3**(6), 273–281 (2013)

[20] Sommervogel, L.: Various models for faults in transmission lines and their detection using time domain reflectometry. Progress In Electromagnetics Research C **103**, 123–135 (2020)

[21] Truong, T.K.: Twisted-pair transmission-line distributed parameters. EDN Mag (2000)

[22] Wheeler, K.R., Kurtoglu, T., Poll, S.D.: A survey of health management user objectives related to diagnostic and prognostic metrics. In: International Design Engineering Technical Conferences and Computers and Information in Engineering Conference. vol. 48999, pp. 1287–1298 (2009)